Materials Research. 2015; 18(6): 1414-1425
DOI: http://dx.doi.org/10.1590/1516-1439.058815

Development and Applications of Highly Functional Al-based Materials by Use of Metastable Phases

Akihisa Inoue[a,b,c]**, Fanli Kong[b], Shengli Zhu[a], Chain Tsuan Liu[d], Fahad Al-Marzouki[c]

[a]*School of Materials Science and Engineering, Tianjin University, Tianjin, China*
[b]*International Institute of Green Materials, Josai International University, Togane, Japan*
[c]*Department of Physics, King Abdulaziz University, Jeddah, Saudi Arabia*
[d]*Center of Advanced Structural Materials, City University of Hong Kong, Hong Kong, China*

Received: October 1, 2015; Revised: November 5, 2015

This paper reviews the features of alloy components, structure and mechanical properties, physical and chemical properties of metastable Al-based alloys developed by use of various liquid or vapor quenching-induced phases such as amorphous, quasicrystalline, nanocrystalline, nanocomposite, supersaturated solid solution and structure gradient phases. As advantages of the metastable Al-based alloys, one can exemplify a high tensile strength of 1500 MPa for amorphous alloys, high elevated temperature strength of 364 MPa at 573 K for nanoquasicrystalline alloys, high strength of 1000 MPa at room temperature and 520 MPa at 473 K for nanocrystalline alloys, relatively high strength of 596 MPa with large elongation of 16% for nanocomposite alloys and high strength of 900 MPa and distinct elongation of 5% for supersaturated fcc-Al solid solution. These highly functional properties, which have not been obtained for conventional crystalline Al-based alloys, have enabled the commercialization of metastable Al-based alloys as structural, machinery and sporting goods materials. Owing to the significant increase of various fundamental properties caused by the essential differences in the structures, the engineering importance of the metastable Al-based alloys is expected to increase steadily in the future low carbon and nature harmonious society.

Keywords: *aluminium alloys, metastable phases, mechanical properties*

1. Background and Objectives

In recent years, there has been a strong demand of developing advanced structural materials with functional properties such as high specific strength, high elevated temperature specific strength, high fatigue specific strength, low corrosion loss and low wear loss. This is because the practical uses of these functional structure materials are expected to cause the saving of material amount, reductions of material cost and energy during material production as well as the saving of consuming energy during practical uses. Besides, the light-weight materials with high corrosion resistance and high wear resistance are effective for the increase of endurance limit and the lightening of final products. Thus, the development of novel Al-based alloys having simultaneously the above-described functional properties is particularly important nowadays.

As strengthening mechanisms for Al-based alloys, the following seven mechanisms are generally known[1]: solid solution, grain size refinement, work hardening, age hardening, precipitation, dispersion and defect-induced solute segregation. We have also noticed that the use of rapid quenching enables highly supercooled liquid solidification in conjunction with a high nucleation rate and low growth rate. By utilizing the high nucleation rate and low growth rate phenomenon, we have synthesized various kinds of metastable phases which change from nanocrystalline base structure to bulk glassy base structure through an amorphous base structure with increasing quenching effect (cooling rate). It is also known that the quenching effect is dominated by cooling rate from melt resulting from rapid solidification processes as well as by supercooling capacity of alloy liquid depending on alloy component and composition.

When we focus on the strengthening caused by metastable phases, the effect is due to the combination of solid solution + ultra-high density of defects for amorphous phase and dispersion + grain size refinement + segregation for nanocrystalline phase. The amorphous plus nanocrystalline mixed phase alloys are expected to have simultaneously almost all the strengthening mechanisms. By utilizing the combined strengthening mechanisms of these metastable phases, we have tried to prepare novel Al-based alloys with the high tensile strength exceeding 1500 MPa at room temperature, high elevated temperature strength above 500 MPa at 573 K, high rotating beam fatigue strength above 400 MPa at 10^7 cycles, high elevated temperature fatigue strength above 100 MPa at 673 K after 10^6 cycles and high corrosion resistance below 20 mm/year in 0.25 M NaOH aqueous solution at 293 K. In addition, these Al-based alloys have been requested to exhibit a low wear loss, low coefficient of thermal expansion and low material density etc. This paper presents the review of the development achievements of metastable Al-based alloys obtained in our group on the basis of the above-described backgrounds and objectives.

*e-mail: ainouebmg@yahoo.co.jp

2. Al-based Amorphous Alloys

The first synthesis of ductile Al-based amorphous alloy was made in 1987 for Al-Ni-Si system by Inoue et al.[2]. The amorphous alloys containing more than 70 at% of Al exhibit a good bending ductility and tensile fracture strength (σ_f) of about 440 MPa. Besides, the amorphous alloys show a unique feature of distinct double halo rings in their electron diffraction patterns, suggesting the phase separation of the glassy phase. Similar double halo rings and peaks have subsequently been found in many Al-based alloy systems such as Al-Ni-Ce, Al-Mn-Si and Al-Mn-Ge etc[2,3]. Such phase separation behavior has been interpreted to result from a significant difference in the heats of mixing between Al-TM (Ni, Mn) and Al-Si or Al-Ge[2,3].

Since the discovery of Al-based amorphous alloys by rapid quenching[2], we have performed a systematic study on the development of Al-based amorphous alloys with the aim of producing novel engineering Al-based alloys with high specific strength. In 1988, we have reported that an amorphous phase is formed even in Al-Ln (Ln = lanthanide metal) binary system[4]. The crystallization temperature (T_x) increases with increasing Ln content and reaches about 505 K at 12% Sm even for the binary amorphous alloys. The addition of the late transition metals (LTM) such as Fe, Co, Ni and Cu to Al-Ln binary alloys was found to be very effective in extending the composition range where an amorphous phase is formed, as exemplified in Figure 1[3]. The effectiveness is the largest for Ni and no distinct difference in the effectiveness among the other three LTM elements is recognized for Al-Ln (Y, La or Ce)-LTM systems. The T_x of these amorphous alloys increase almost linearly with increasing Ln content and reach about 750 K at 15% Ln content. The T_x level is the highest for LTM = Fe and Co,

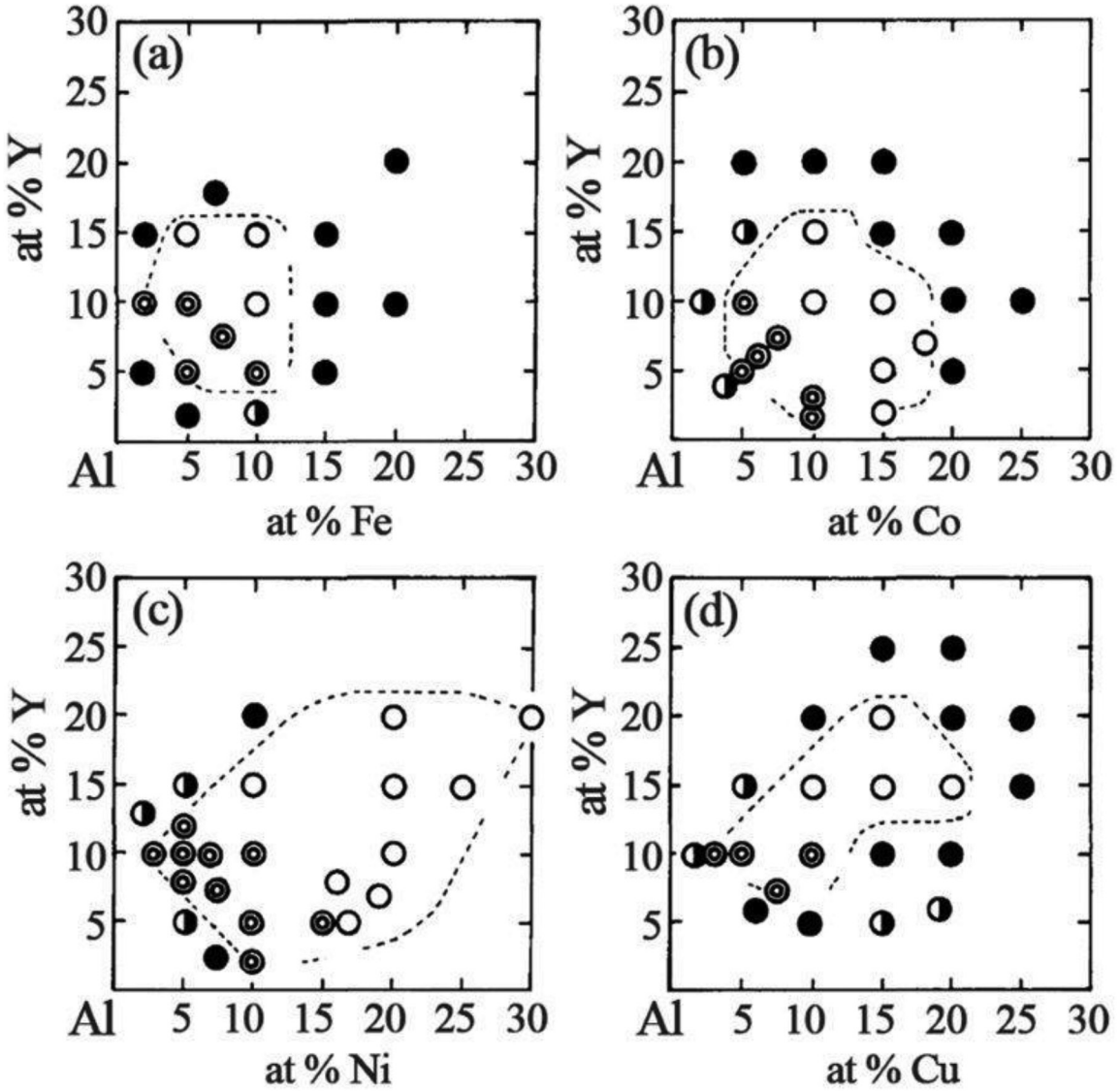

Figure 1. Compositional range for formation of amorphous phase in (a) Al-Y-Fe, (b) Al-Y-Co, (c) Al-Y-Ni and (d) Al-Y-Cu systems: (◎) amorphous (ductile); (○) amorphous (brittle); (◑) amorphous plus crystalline; (●) crystalline[3].

followed by Ni and then Cu. Besides, we can recognize a linear relationship between E and T_x, H_v or σ_f for Al-Y-Ni amorphous alloys[5]. The highest tensile strength of Al-Y-Ni amorphous alloys reaches 1140 MPa[5]. Similar Al-based amorphous alloys with a good ductility were also found in Al-TM-RE (where TM = transition metals, RE = yttrium and rare earths) system by S. J. Poon et al.[6-8].

The additional effect of the fourth TM (TM=Transition Metal) element to Al-Y-Ni and Al-Ce-Ni amorphous alloys was examined by choosing Zr, V, Nb, Cr, Mn, Fe, Co, Ni or Cu as TM element[9]. The Co, Fe and Ni elements were found to be useful for further extension of amorphous phase region in $(Al_{0.85}Ni_{0.05}Y_{0.10})_{100-x}M_x$ and $(Al_{0.84}Ni_{0.10}Ce_{0.06})_{100-x}M_x$ alloys. The H_v increases significantly with increasing the M content and the highest H_v reaches about 500 for M=Mn or Ni, as shown in Figure 2[9]. The most favorable quaternary Al-based alloy with a good bending ductility was decided to be $Al_{85}Ni_5Y_8Co_2$ and the tensile strength, E and H_v of the amorphous alloy were 1250 MPa, 74 GPa and 350, respectively, as summarized in Table 1. In addition to Al-Ln-TM systems, the amorphous alloys with a good bending ductility were formed in Al-Ni-ETM (ETM=Zr, Hf, Nb) ternary alloys and their amorphous alloys also exhibited rather high tensile fracture strength reaching about 800 MPa[10,11]. Fundamental properties such as electrical resistivity and Hall coefficient also show a distinct compositional dependence. For instance, there is a clear tendency for electrical resistivity at room temperature of $Al_{90-x}Y_{10}TM_x$ amorphous alloys to increase from 0.7 to 2.3 μΩm with increasing TM content. Here it is important to note that the Al-Ln-LTM amorphous alloys exemplified for $Al_{85}Y_{10}Ni_5$ exhibit glass transition in the temperature range before crystallization. The glass transition can be recognized by the increase in specific heat, steep decreases in Young's modulus and tensile fracture strength, and drastic increase in elongation etc. Thus, Al-based amorphous alloys in the Al-Ln-LTM system can be classified as a glass type alloy. These glassy alloys have also been recognized to exhibit a much better corrosion resistance than those for pure Al and Al-Cu-Mg (2024) alloys in NaOH and HCl aqueous solutions at 298 K[12].

Subsequently, Inoue et al. have found that the addition of Sc to Al-Y-Ni-Co amorphous alloys is very effective for improvements of H_v and σ_f[13]. The H_v and σ_f increase almost linearly with increasing Sc content and reach about 450 and 1504 MPa, respectively, at 5% Sc, as shown in Figure 3. The 5%Sc-containing glassy alloy exhibits a good bending ductility and can be bent through 180 degrees without fracture. The tensile fracture takes place along the maximum shear stress plane and the fracture surface consists of well-developed smooth and vein patterns. Furthermore, a number of shear slip steps are observed in the region just near the fracture surface edge, indicating that the Al-Y-Ni-Co-Sc glassy alloy has a good ductile nature in spite of the high tensile strength exceeding 1500 MPa. It is also noticed that the specific tensile strength of σ_f/ρ for the glassy alloy exceeds 4.4×10^5 Nm/kg[13].

In addition to amorphous alloys in a ribbon form, Al-based amorphous alloy wires with a circular cross section have also been produced in the diameter range up to 100 μm by the melt extraction method. For instance, $Al_{85}Ni_{10}Ce_5$ amorphous alloy wire of 70 μm in diameter has a good bending ductility and can be bent through 180 degrees without fracture, as shown in Figure 4. Besides, the wire exhibits high tensile fracture strength of 930 MPa[14].

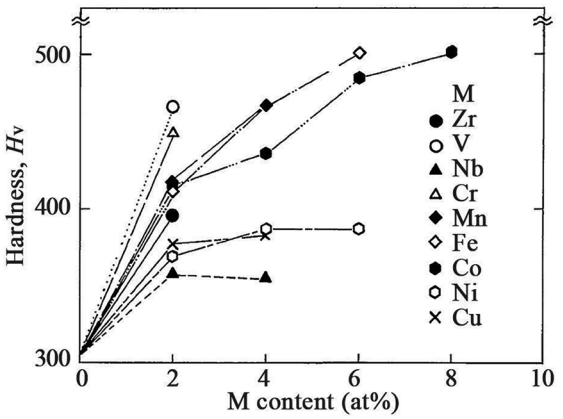

Figure 2. Changes in Vickers hardness (H_v) of $(Al_{0.85}Ni_{0.05}Y_{0.10})_{100-x}M_x$ (M=Zr, V, Nb, Cr, Mn, Fe, Co, Ni or Cu) amorphous alloys with an increase of the M content[9].

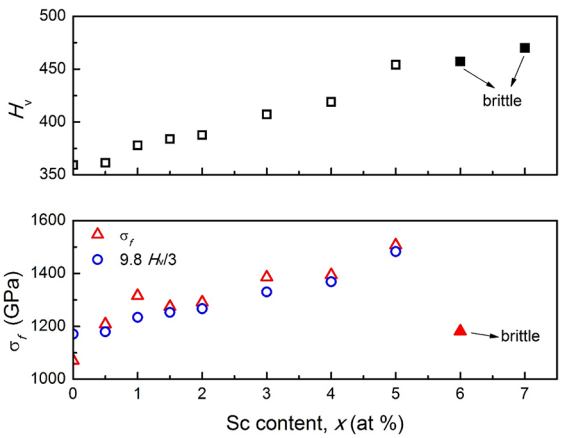

Figure 3. Vickers hardness and tensile strength values as a function of Sc content in $(Al_{0.64}Y_{0.09}Ni_{0.05}Co_{0.02})_{100-x}Sc_x$ amorphous alloys[13]. The alloys which are brittle are shown by solid symbol.

Table 1. Mechanical properties of Al-Ni-Y and Al-Ni-Y-Co amorphous alloys[9].

Alloys	σ_f (GPa)	E (GPa)	H_v	ε_t (%)	$\varepsilon_{c,y}$	$\sigma_{c,y}$ (MPa)
$Al_{85}Ni_5Y_{10}$	920	62.8	310	1.4	0.016	1010
$Al_{85}Ni_5Y_8Co_2$	1250	74.0	350	1.7	0.015	1145
$Al_{85}Ni_5Y_7Co_3$	1140	71.2	340	1.5	0.016	1110

Tensile fracture strength (σ_f), Young's modulus (E), Vickers hardness (H_v), tensile fracture strain (ε_t), compressive yield strain ($\varepsilon_{c,y} \approx 9.8H_v/3E$) and compressive yield strength ($\sigma_{c,y} \approx 9.8H_v/3$).

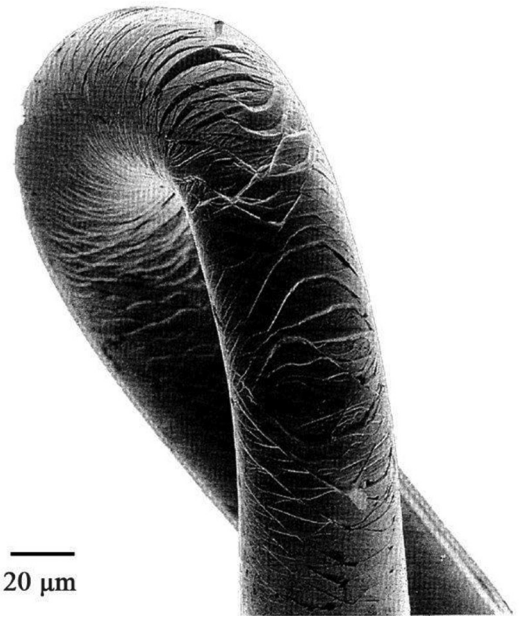

Figure 4. Scanning electron micrograph revealing the deformed structure of an $Al_{85}Ni_{10}Ce_5$ wire which was bent through 180 degrees[14].

Much effort has also been devoted to produce thick sheets of Al-based glassy alloys by developing an incremental quenching technique consisting of high pressure gas atomization, followed by incremental impact deposition on rotator. The thickness is in the range of about 0.12 to 7 mm and no crystalline phases are recognized in the X-ray diffraction patterns obtained from their sheets[15]. The formation of such thick sheets has been attributed to the incremental stacking of flattened powder. This is significant contrast to the small thickness (<1 mm) for Al-based alloys produced by conventional melting and casting.

If we can avoid the stacking of the powders which are flattened by the impact of spherical liquid droplets onto the rotator, there is a possibility of producing flaky powders which have not been obtained up date by the direct production method from liquid. Based on this concept, we developed a two-stage quenching technique in which the supercooled liquid droplets with very fast moving velocity produced by high pressure gas atomization can be flattened onto a rapidly rotating wheel[16]. The resulting Al-based flaky powders have very thin thickness of about 0.5 to 4 μm and large aspect ratios of 20 to 300 and exhibit very smooth outer surface with good metallic luster, as shown in Figure 5. The two-stage quenching method also has an advantage of producing glassy alloy powders over the whole powder size range because all the spherical supercooled liquid droplets, which could not solidify to a glassy phase in the first solidification process of high pressure argon gas atomization, are solidified to a glassy phase by the subsequent impact flattening, followed by depatching the flattened powder from the rotator by centrifugal force. We have also confirmed that the flaky Al-based glassy powder is suitable for application to a surface coating material because of its good metallic luster, thin thickness with large aspect ratio, high hardness, good bending ductility and high corrosion resistance[17,18].

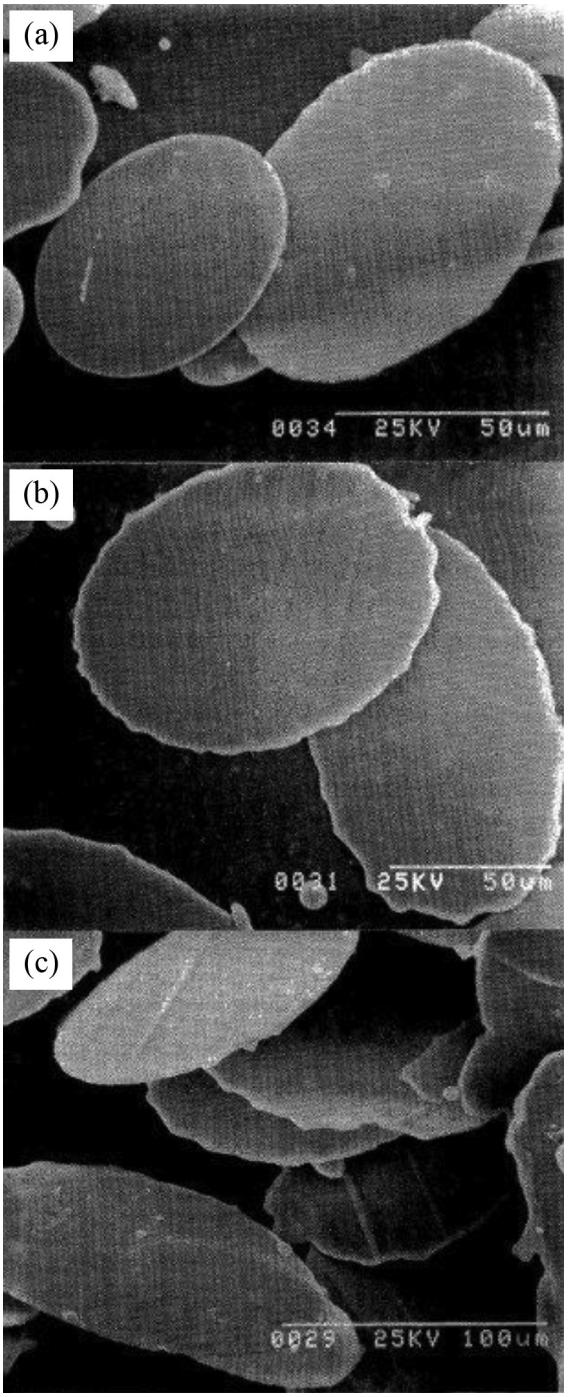

Figure 5. Scanning electron micrographs revealing effect of size fraction on morphology in $Al_{85}Ni_{7.5}Mm_{7.5}$ powder produced by the two-stage quenching method. (a) 25 to 45 μm, (b) 45 to 63 μm, (c) 63 to 75 μm[16].

3. Bulk Glassy Alloys

It is important to obtain Al-based BMGs exhibiting high strength, good ductility and high corrosion resistance. By using the injection casting technique to copper mold, we produced glassy Al-based alloys in a sheet form with thickness up to 0.3 mm[19]. The increase in the thickness to

0.4 mm caused the coexistence of crystalline phase in the central region, though a glassy phase region is recognized in the edge region. We further tried to produce a thicker glassy alloy sheet by using a die-mold casting technique[20]. A nearly glassy phase was formed in the surface region of the sheets with a thickness up to about 3 mm, though the complete suppression of crystalline phase is difficult in the thick range of 0.5 to 3 mm. The production of the thick sheets with glassy surface coated layer seems to be important for future application as high specific strength, high surface hardness and high corrosion resistant materials in bulk form.

Very recently, Zhang et al. have reported that a mostly glassy alloy rod with a diameter of 1 mm is formed through the addition of 0.5%Sc to Al-Ni-Y-Co base alloy by the copper mold casting method, though a tiny amount of fcc-Al phase is detected only in the central region of the rod[21]. The alloy rod exhibits a high compressive yield strength of about 1200 MPa and plastic strain of about 2.4% in compression. A large number of shear bands can be observed on the lateral surface. With further increasing rod diameter to 1.5 mm and 2 mm, crystalline phases precipitate out in the central region of the rod and the yield strength decreases significantly in conjunction with the distinct change from ductile fracture surface mode for the 1 mm rod to brittle fracture mode for the 1.5 and 2 mm rods[21].

We further challenged to produce Al-based BMGs through the modification of alloy component for Al-Y-Ni-Co alloy. In the challenge, Domitri et al. have noticed that the 2% Ca addition increases the reduced glass transition temperature (T_g/T_l) value from ~0.55 at 0%Ca to 0.613 at 2% Ca through the increase of T_g and the decrease of T_l[22]. Besides, the 2% Ca-containing amorphous alloy has been reported to have an activation energy for crystallization of about 311 kJ/mol which is much higher than those for other known Al-based glassy alloys. Based on the knowledge of the high T_g/T_l value and the difficulty of crystallization, we have tried to produce a bulk glassy alloy by the injection casting technique. However, we could not produce any bulk glassy alloy with a diameter of 1 mm because of the difficulty of suppressing the precipitation of Al_4Ca phase. The easy precipitation of Al_4Ca is presumably due to a much larger negative heat of mixing for Al-Ca pair as compared with those for other atomic pairs of Ca-Y, Ca-Ni and Ca-Co[21].

4. Al-based Nanocrystalline Alloys

When Al-rich Al-Ln-TM alloys containing about 88 at% are selected, their amorphous alloys crystallize through two exothermic peaks[23-25]. The first broad peak is due to the precipitation of nanoscale fcc-Al phase with a grain size of 3 to 10 nm. When the amorphous alloy is annealed in the first broad exothermic peak temperature range, the annealed alloy consists of nanoscale fcc-Al phase surrounded by the remaining amorphous phase. The precipitation of nanoscale fcc-Al phase causes significant increases of H_v, E and σ_f. For instance, as shown in Figure 6, the $Al_{88}Ni_9Ce_2Fe_1$ nanocrystalline alloys exhibit the maximum σ_f of 1560 MPa at about 25% volume fraction (V_f) of fcc-Al phase in conjunction with high H_v of 403 and E of 71 GPa[25]. The fracture surface of the nanocrystalline alloy ribbon shows a well-developed ledge pattern with much larger surface ruggedness, indicating a

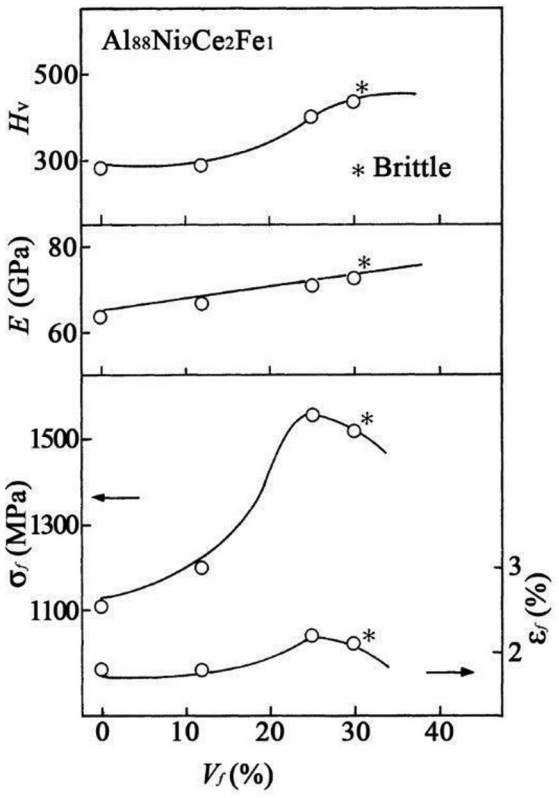

Figure 6. Hardness (H_v), Young's modulus (E), tensile fracture strength (σ_f) and fracture elongation (ε_f) as a function of volume fraction of fcc-Al phase (V_f) for melt-spun $Al_{88}Ni_9Ce_2Fe_1$ amorphous alloys[25].

significant increase of ductility by the existence of nanoscale fcc-Al phase. The significant increase in tensile fracture strength is presumably because the nanoscale fcc-Al phase can act an effective resistance medium to shear sliding of the glassy phase. The nanocrystalline alloy also exhibits a high heat resistant strength of about 950 MPa even at 573 K as well as the improvement of ductility. There is a good linear relation for H_v to increase with increasing volume fraction of fcc-Al phase[25]. The relation agrees well with the result obtained by the simple mixture rule.

Here it is important to investigate the reason why the nanoscale fcc-Al phase can increase the tensile fracture strength of the nanocrystalline alloy. The significant increase implies that the strength of nanoscale fcc-Al phase is much higher than that for the glassy matrix. The reason for such a high strength of the nanoscale Al phase has been thought to be due to the following two factors, i.e., (1) defect-free perfect crystal structure, and (2) highly defected crystal structure. The former mechanism was proposed about 20 years ago[26]. However, recent HRTEM data shown in Figure 7 indicates the existence of an ultra-high density of dislocations inside fcc-Al phase and the density reaches as high as the order of $10^{24} \sim m^{-3}$[27]. The introduction of such a high density of dislocations in the nanoscale Al phase may be due to the generation of residual internal stress caused by the difference in thermal expansion of coefficient and the imperfect formation of fcc-Al crystal structures from icosahedral-like atomic configurations.

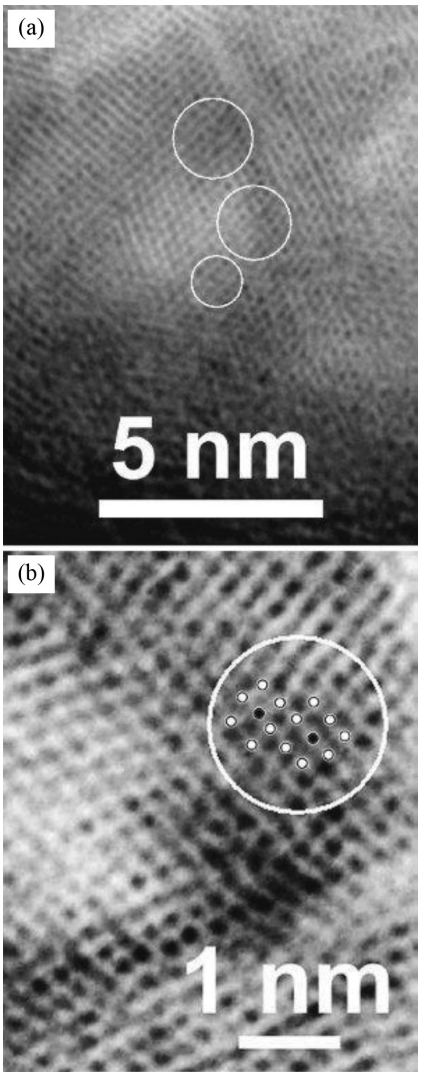

Figure 7. High-resolution TEM images of the $Al_{85}Y_4Ni_5Co_2Pd_4$ glassy alloy in as-solidified state[27].

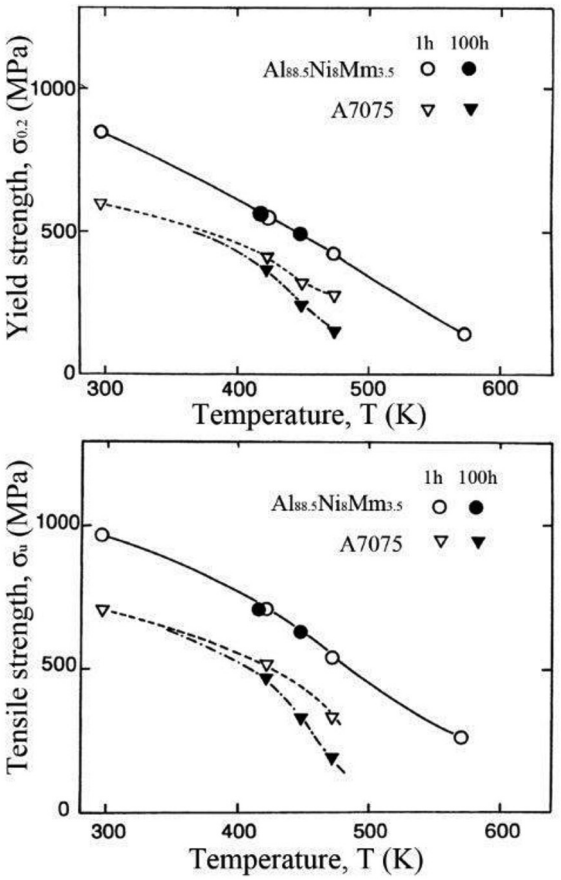

Figure 8. Temperature dependence of tensile yield strength ($\sigma_{0.2}$) and ultimate tensile strength (σ_u) for as-extruded $Al_{88.5}Ni_8Mm_{3.5}$ alloy annealed for 1 and 100 h at each testing temperature. The data for the A7075 alloy are also shown for comparison[29].

By use of a spray-forming technique, fully dense nanocrystalline plates of Al-Y-Ni-Co-Si-La alloys were produced in the disc plate with a diameter of 200 mm and a thickness up to 12 mm[28]. The plates have the nanocrystalline structure of glassy and fcc-Al phases in the middle region. The nanocrystalline plates have rather high H_v of about 420 and high E of about 80 GPa. These H_v and E values are independent of the position in the sheet[28].

By warm extrusion of atomized powders consisting of amorphous plus fcc-Al phases, we can obtain fully dense bulk nanocrystalline alloys consisting of fcc-Al phase with grain size of about 200 nm including homogeneously dispersed particles with sizes of 50 to 200 nm[29]. The extruded bulk nanocrystalline alloys exhibit a high yield strength of about 850 MPa, high tensile strength of about 1000 MPa as well as a rather high elevated temperature strength of 250 MPa at 573 K which are much superior to those for A7075 alloy, as shown in Figure 8. The bulk nanocrystalline alloys also exhibit a rather high rotation beam fatigue strength of 330 MPa after 10^7 cycles. It is thus concluded that the nanocrystalline alloy has a higher fatigue strength and higher tensile strength than those for conventional Al-based alloys and newly developed Al-based alloys produced by powder metallurgy processes[1,29]. The nanocrystalline alloys also have lower thermal expansion coefficient and lower wear losses than those for A6061, A5056 and A-17mass % Si alloys.

The nanocrystalline structure had rather high thermal stability and kept fine grain size of about 1 μm even after annealing for 30 min at 873 K[30]. The rather high nanocrystalline structure stability has enabled the appearance of superplasticity with m value of 0.3 to 0.5 and elongation of about 500%, indicating that the superplastic forming process can be applied to the bulk nanocrystalline alloys. In particular, bulk nanocrystalline Al-Ni-Mm-Zr alloy with grain size of 120 nm exhibits good combined properties, e.g., 830 MPa for the yield strength, 890 MPa for the tensile strength, 96 GPa for E and 4 to 9% for elongation[31]. The yield strength obeys well the Hall-Petch relation which can be presented by $\sigma_{0.2} = 489 + 3.65d^{-1/2}$. This relation is significantly different from that ($\sigma_{0.2} = 5 + 2.30d^{-1/2}$) for conventional Al-based alloys[32]. The significant difference indicates that the strengthening mechanisms are significantly

different between the bulk nanocrystalline and conventional Al-based alloys, in agreement with the phenomenon expected in the section of background.

5. Al-based Nanocomposite Alloys

For an Al-rich $Al_{95}Zr_1Ni_1Mm_3$ alloy, it has been found that the atomized powder of about 250 μm in diameter has a unique solidification structure in which a primary precipitation phase of Al_3Zr is surrounded by eutectic Al + $Al_{11}Mm_3$ phases, as exemplified in Figure 9[33]. The grain sizes of each constituent phase are much smaller than those for commercial powder metallurgy Al alloys such as SUMIALTOUGH and A390, in spite of much higher Al composition. The bulk nanocomposite Al-Zr-Ni-Mm alloy produced by warm extrusion of the atomized powders with the unique solidification structure keeps a high hardness above 84 in the temperature range up to 773 K and exhibits a rather high yield strength of about 530MPa at room temperature, 210 MPa at 573 K and 100 MPa at 673 K. In addition, the nanocomposite alloy exhibits a high elevated temperature fatigue strength of 190 MPa at 423 K and 160 MPa at 473 K after 10^6 cycles which are much superior to those for commercial AC8A-T7 alloy. It is noticed that the nanocomposite bulk alloy keeps high fatigue ratios of about 40 in a wide temperature range up to 673 K. The alloy also exhibits high impact fracture energy of 15 to 25 ~ J/cm^2[33]. It is thus said that the nanocomposite alloys of $Al_{95}Zr_1Ni_1Mm_3$ and $Al_{95}Zr_1Mm_4$ possess favorable combination of good static and dynamic mechanical properties and have been commercialized as heat resistant Al-based materials even at present.

6. Al-based Nano-quasicrystalline Alloys

It is known that the quasicrystalline phase has a number of advantages such as low growth rate, high resistance to elastic and plastic deformations, high heat-resistant strength, high wear resistance, low coefficient of thermal expansion, low thermal conductivity, isotropic properties, pseudo spherical morphology, Al-rich composition, isolated homogeneous dispersion surrounded by Al, dissolution of many solute elements and high corrosion resistance etc[34-36]. By utilizing these advantages, we have been trying to develop a new type of Al-based alloy containing quasicrystalline phase as a main constituent phase[37]. For instance, the as-spun structure of $Al_{94}V_4Fe_2$ alloy changed from Al + amorphous to quasicrystalline (Q) phases through Al + amorphous + Q phases with decreasing cooling rate, as shown in Figure 10[38]. The as-spun alloy ribbon exhibited the maximum tensile fracture strength of about 1400 MPa in the structure state of Al + Am + Q phases. The size was as small as 50 to 100 nm for the fcc-Al and 10 to 80 nm for the Q phase[38].

Such a mixed structure of fcc-Al + Q phases has been reported to be formed in as-atomized powders and as-extruded bulk forms from atomized powder for a number of Al-based alloys such as Al-Fe-Cr-M (M=Ti or V)[39], Al-Cr-Ce-M[40], Al-Mn-Cu-M[41] and Al-Cr-Cu-M[41] systems. The nano-Q bulk alloys can be classified to the following three types,

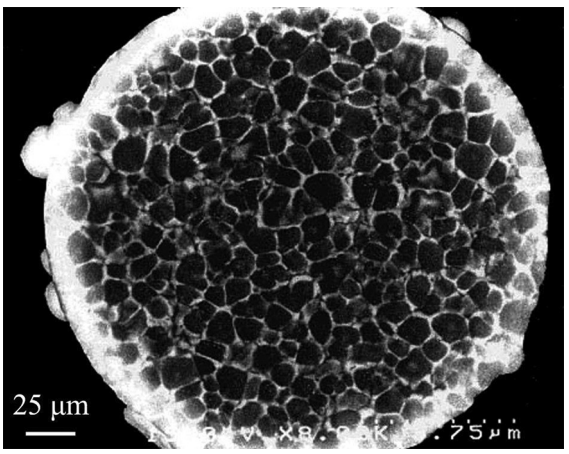

Figure 9. Scanning electron micrograph of atomized $Al_{95}Zr_1Ni_1Mm_3$ alloy powder[33].

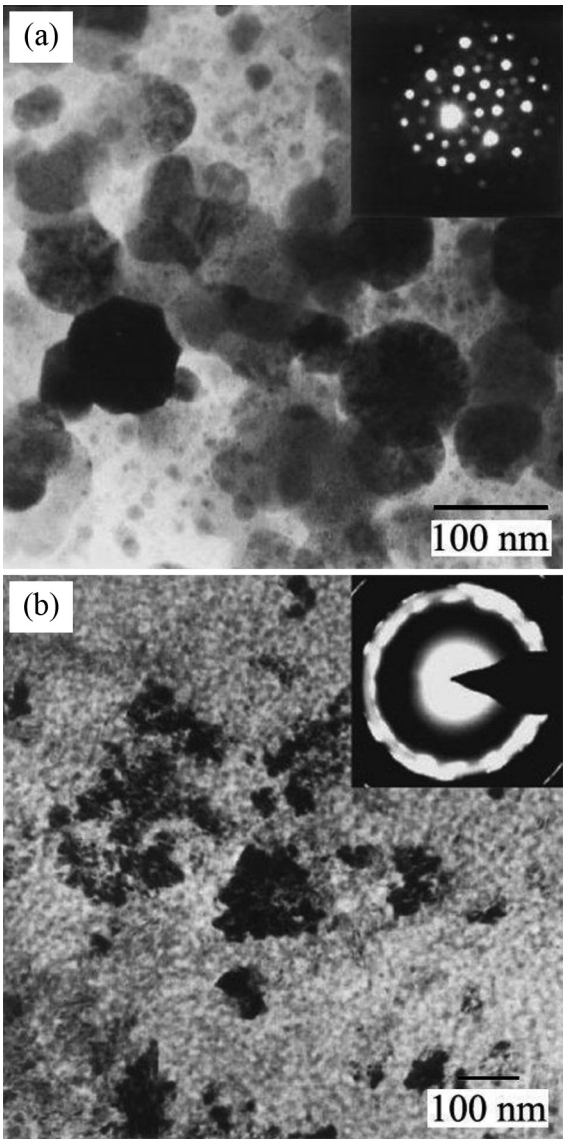

Figure 10. Bright field TEM images of $Al_{94}V_4Fe_2$ alloy melt-spun at (a) 20 and (b) 50 m/s. The inset of (a) is the microdiffraction pattern obtained from an i-phase particle and that of (b) is the selected area diffraction pattern from the alloy melt-spun at 50 m/s[38].

(1) high-strength type of Al-Cr-Ce-Ti (or V) and Al-Mn-Ce alloys with tensile strength of 600 to 800 MPa and elongation of 5 to 10%, (2) high-ductility type of Al-Mn-Cu-Ti (or V) and Al-Cr-Cu-Ti (or V) alloys with a tensile strength of 500 to 600 MPa and elongation of 12 to 30%, and (3) high-elevated temperature strength type of Al-Fe-Cr-Ti alloys with tensile strength of 350 MPa at 573 K[42].

Based on the above-mentioned basic knowledge that Al-Fe-Cr-Ti alloys have the high elevated temperature strength[43], much effort was devoted to develop a new type of heat resistant strength alloys with better performance in collaboration with Honda Research & Development Corporation[44] because there have been strong needs for high strength and heat resistant materials for automobile industries. We examined the additional effect of TM elements on the formation tendency of nano-Q structure in $(Al\text{-}Fe\text{-}Cr\text{-}Ti)_{100-x}Co_x$ alloys. As a result, it has been clarified that the addition of 3% Co causes the change to amorphous phase and the 2% Mo addition is effective for the refinement and homogeneized dispersion of the Q phase. Therefore, we have decided that the most suitable alloy composition is $Al_{93}Fe_{2.45}Cr_{2.45}Mo_{0.5}Ti_{0.8}Co_{0.8}$. The extruded bulk alloy was produced in the following extrusion condition; (1) powder size was below 150 μm, (2) degassing was made for 3 h at 573 K in vacuum, (3) heating was made for 1 h at 673 K and (4) warm extrusion ratio at 673 K was 11. The Q particles in the extruded bulk alloy have a size of about 100 nm and about 75% volume fraction. The extruded alloy exhibits a high tensile strength of 710 MPa at room temperature, 364 MPa at 573 K and 203 MPa at 673 K, all of which are much higher than those for A2618-TC. The alloy also exhibits high elevated temperature fatigue strength of 100 MPa at 623 K after 5×10^6 cycles under uniaxial tension-compression load. The nano-Q alloy also exhibits lower specific wear rate of 2.8×10^{-7} mm^2/kg at the sliding velocity of 2 m/s, higher E of 72 GPa at 673 K and lower thermal expansion coefficient of 22×10^{-6} K^{-1} at 673 K as compared with commercial A2618-T6 alloy.

The formability of the extruded alloy was also examined by compression test at a strain rate of 0.78 s^{-1} at 673 K. After 60% compression strain, neither crack for the deformed alloy nor grain growth of Q phase was observed. The nano-Q alloy exhibits higher tensile strength values at room temperature and elevated temperatures of 473 to 673 K, higher wear resistance, higher Young's modulus and lower coefficient of thermal expansion in comparison with A2618-T6 alloy, though the elongation is lower and the density is higher. The newly developed nano-Q Al-Fe-Cr-Ti-Co-Mo alloy has been tested for applications to some heat-resistance parts in automobiles at present.

Here it is important to describe that the development of new Al-based alloys by use of the homogeneous dispersion of nanoscale quasicrystalline phase surrounded by the fcc-Al phase has been carried out at present in many countries[45-48] by the trigger effect of our data[34,37-41].

7. Al-based Alloys Reinforced with Bulk Glassy Alloys

The reinforcement of Al crystalline alloys with bulk glassy alloys is expected to enable the production of novel Al-based alloys with features of inexpensive PM metallurgy process, high specific strength, good ductility and material weight reduction. We chose three kinds of bulk glassy alloys, i.e., $Cu_{54}Zr_{36}Ti_{10}$, $[(Fe_{0.5}Co_{0.5})_{0.75}B_{0.20}Si_{0.05}]_{96}Nb_4$ and $Fe_{72}B_{14.4}Si_{9.6}Nb_4$, because their T_g are comparable to T_m of Al[49-51]. By sintering the mixture of Al powder and the FeCo-based glassy alloy powder at around T_g, fully dense composite alloys are produced and exhibit a rather high compressive yield strength of about 600 MPa in conjunction with large strain of about 12%[51]. The yield strength level is comparable to weight reduction by about 60%. The simple production method to produce the Al-based bulk alloy with high strength and high ductility is attractive for future development of new PM Al-based composite alloys.

8. Vapor-deposited Al-based Alloys

By using a two-target electron-beam evaporation equipment, vapor-deposited Al-based alloy sheets in a form of 120 × 120 × 1 mm were formed in Al-TM (TM=Fe, Zr, Ni, Ti, Cr) systems[52-54]. For instance, the Al-Fe deposited sheets consist of fcc-Al solid solution saturated with Fe and the fcc-Al phase has a grain size of about 2 μm at about 1%Fe, about 200 nm at 1.3%Fe and about 20 to 40 nm at 2.6 and 3 at% Fe[52]. Thus, the grain size decreases drastically in the vicinity of 1.5 to 2 at% Fe. The 0.9 to 2.2% Fe alloy sheets exhibit high H_v of about 220 to 260, high yield strength of 700 to 900 MPa and elongation of 5 to 9%, as shown in Figure 11. The highest tensile strength attained was about 1000 MPa at 2.6% Fe and the H_v of the 2.6% Fe alloy sheet was about 300. In addition to the high tensile strength, the Al-Fe alloy sheets with 0.9 to 1.2% Fe exhibited high fracture toughness of 65 to 75 MPa·m$^{1/2}$. The best combined properties of tensile strength and fracture toughness were 860 MPa and 75 MPa·m$^{1/2}$, respectively, for the Al-0.9%Fe alloy sheet. Both hardness and tensile strength are proportional to the reciprocal square root of the grain size, as shown in Figure 12. The Al-Fe alloy sheets also show a good Hall-Petch relation even in the high tensile fracture strength level of 700 to 1000 MPa.

The local structure around Fe atom in the vapor-deposited Al-Fe sheets was also examined by the Fe K-absorption edge EXAFS method[55]. The first neighbor atomic distance of the Al-2% Fe alloy sheet agrees well with those for Al_3Fe and Al_2Fe compounds and deviates significantly from that of the fcc-Al phase, indicating the development of Al-Fe short range ordered atomic configurations which can play an important role in the achievement of an ultra-high tensile strength for the Al-Fe deposited sheets.

Similar high strength nanocrystalline alloy sheets were also produced for Al-Zr and Al-Fe-Zr sheets[53]. For instance, the $Al_{95.3}Zr_{4.0}Fe_{0.07}$ alloy sheet of 1 mm in thickness consists of fcc-Al supersaturated solid solution with fine grain sizes of 260 to 680 nm and exhibits a high elevated temperature strength of 800 MPa at room temperature, 536 MPa at 523 K and 434 MPa at 573 K, all of which are much higher than those for 7075-T6 (ESD) alloy. It is thus concluded that the Al-Fe sheet is a high strength and high fracture toughness type, while the Al-Fe-Zr sheet is a high elevated temperature strength type material.

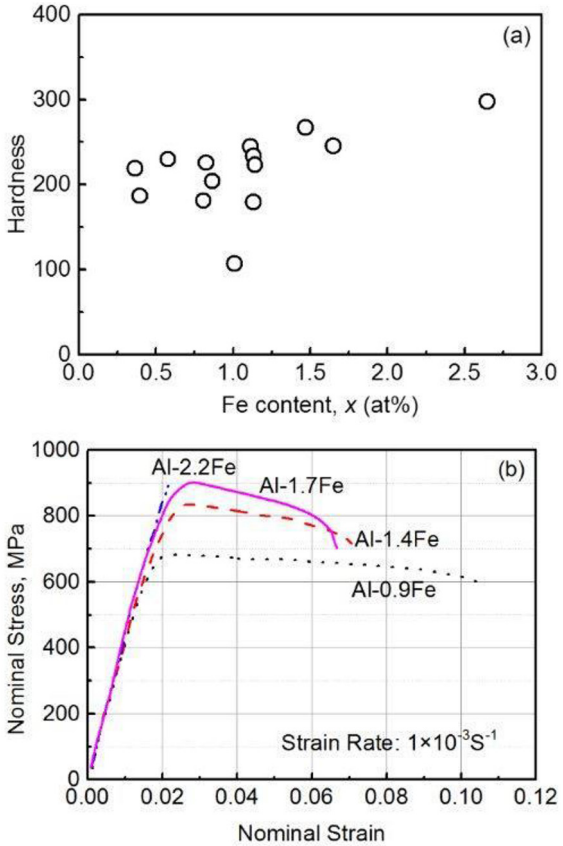

Figure 11. Relationship between (a) Fe content and Vickers hardness and (b) Stress-Strain curve of Al-Fe deposited alloy[52].

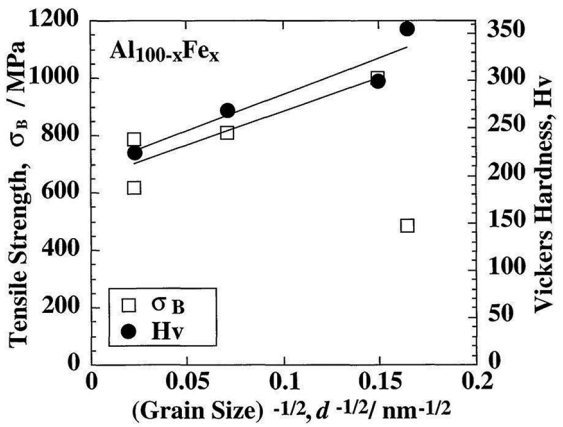

Figure 12. Grain size dependence of tensile strength and Vickers hardness of Al-Fe deposited alloy[52].

9. Structure Gradient Al-based Alloys

By sputtering $Al_{80}Ti_{20}$ and $Al_{80}Zr_{20}$ in a mixed gas atmosphere of Ar + N_2, the structure-gradient Al-based alloy films have been produced[56-58]. For instance, the structure of the Al-Ti alloy films produced by controlling nitrogen partial pressure changes from an fcc-Al supersaturated solid solution

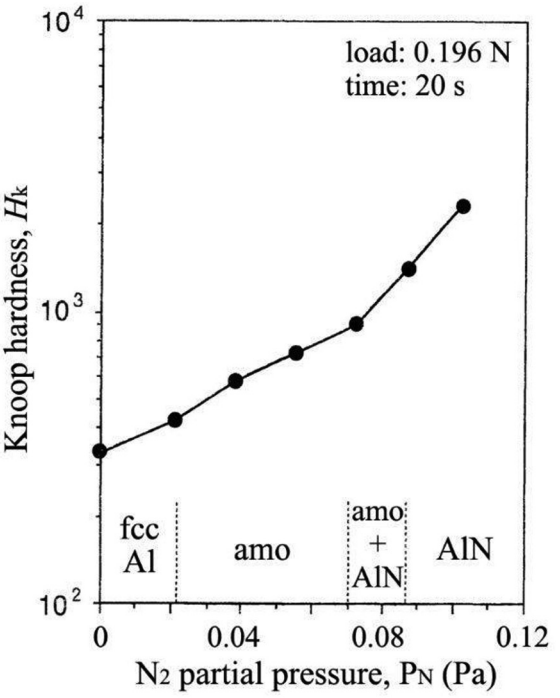

Figure 13. Knoop hardness number (H_k) as a function of PN for the fcc-Al(Ti), amorphous Al(Ti, N), amorphous plus hexagonal Al(Ti)N and hexagonal films[57].

to AlN through amorphous, and amorphous + AlN phases with increasing partial nitrogen pressure from 0 to 0.12[57]. The structural change caused a significant change of Knoop hardness from 325 for Al-phase to 2310 for AlN through 430 to 910 for the amorphous phase, as shown in Figure 13. The amorphous phase had a wide range of Knoop hardness values ranging from 429 to 900 with increasing partial nitrogen pressure from 0.02 to 0.07. Similar changes in the structure and Knoop hardness have also been obtained for $(Al_{0.8}Zr_{0.2})_{100-x}N_x$ alloy films[58].

10. Applications

Bulk nanocrystalline Al-based alloys in Al-Ni-Mm-Zr system with a trademark of GIGAS were commercialized as machinery, structure and sporting goods parts by YKK Corporation[42]. The real application fields were robot parts such as arm, finger and foot, machinery parts, die cast molds, sporting goods such as soft baseball bat, tennis racket and golf club etc., light weight tools, fishing reel, gear in bicycle and wheelchair parts, as exemplified in Figure 14. The achievement of application is due to the simultaneous satisfaction of the high specific strength, high specific modulus, high fatigue limit, low coefficient of thermal expansion, low wear resistance and high corrosion resistance.

The nanocomposite Al-based alloys in the Al-Ni-Mm-Zr system with a trademark of NANOALUMI have also been commercialized as high heat resistant and toughness materials even at present by Sumitomo Electrical Corporation[59].

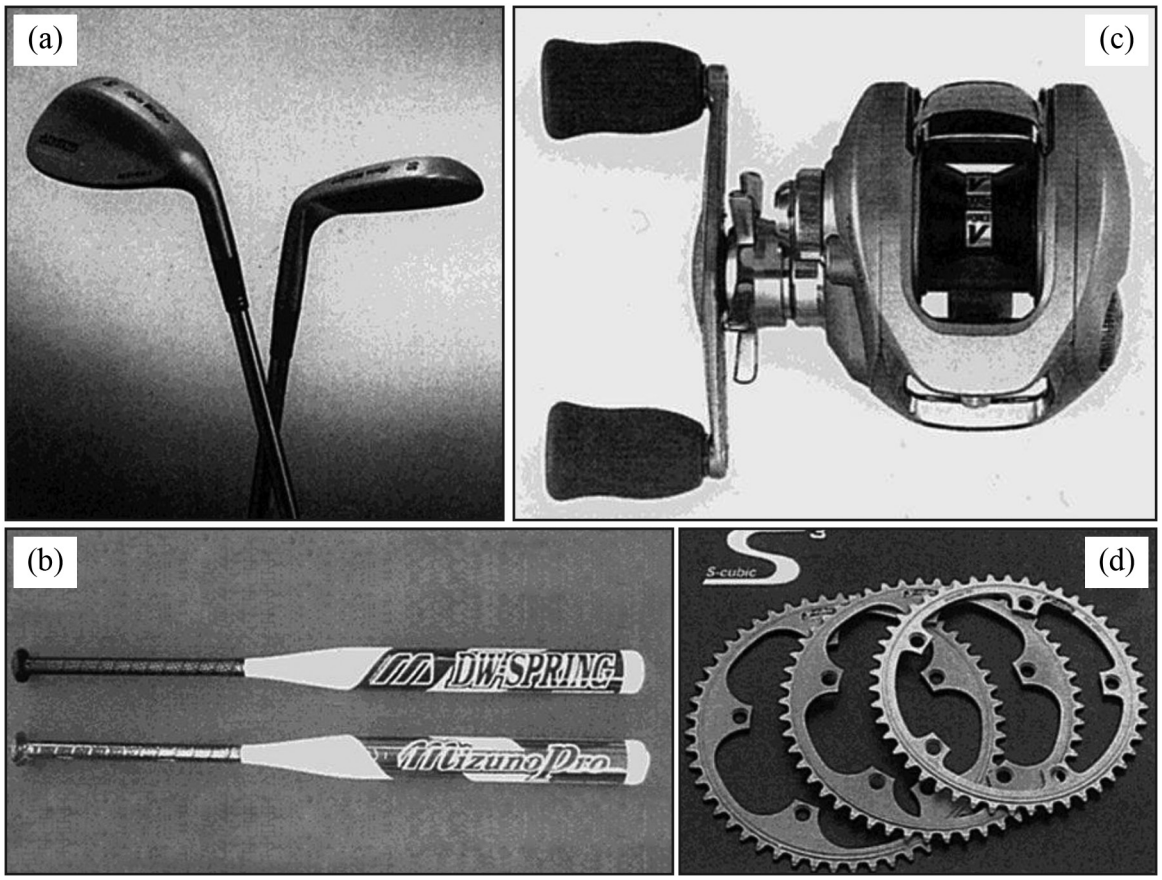

Figure 14. Application examples of nanocrystalline Al-based alloys: sporting goods (a, b), fishing reel (c) and gears in bicycle (d). These data were taken from YKK and Daiwa Corporations[42].

11. Conclusions

We have developed metastable Al-based alloys consisting of amorphous, nanocrystalline and nanoquasicrystalline phases. These new metastable Al-based alloys exhibit high static and dynamic mechanical properties, high elevated temperature strength and good workability which have not been obtained for conventional Al-based crystalline alloys. It is expected that bulk metastable alloys with more functional characteristics and larger material dimensions will be obtained through the fabrication of new structures via novel alloy compositions and production processes. By more effective use of metastable phases, there is a high possibility of commercializing new metastable materials such as higher heat resistant nano-qusicrystalline materials, surface-coated Al-based glassy materials, vapor-deposited Al-based nanocrystalline materials and structure and/or composition gradient materials. It is believed that the further developments of these novel Al-based metastable alloys will contribute greatly to the future sustainable society.

Acknowledgements

The authors would like to acknowledge the financial support of CITIC Dicastal Co. Ltd. China. The authors also acknowledge the Recruitment Program of Global Experts "1000 Talents Plan" of China (WQ20121200052) and Deanship of Scientific Research (DSR), King Abdulaziz University, Jeddah, Saudi Arabia (1-1-1435/HiCi).

References

1. Inoue A and Kimura H. Fabrications and mechanical properties of bulk amorphous, nanocrystalline, nanoquasicrystalline alloys in aluminum-based system. *Journal of Light Metals*. 2001; 1(1):31-41. http://dx.doi.org/10.1016/S1471-5317(00)00004-3.
2. Inoue A, Yamamoto M, Kimura HM and Masumoto T. Ductile aluminium-base amorphous alloys with two separate phases. *Journal of Materials Science Letters*. 1987; 6(2):194-196. http://dx.doi.org/10.1007/BF01728983.
3. Inoue A, Ohtera K, Kita K and Masumoto T. New amorphous alloys with good ductility in Al-Ce-M (M=Nb, Fe, Co, Ni or Cu) systems. *Japanese Journal of Applied Physics*. 1988; 27(10, Part 2):L1796-L1799. http://dx.doi.org/10.1143/JJAP.27.L1796.
4. Inoue A, Ohtera K and Masumoto T. New amorphous Al-Y, Al-La and Al-Ce alloys prepared by melt spinning. *Japanese Journal of Applied Physics*. 1988; 27(5, Part 2):L736-L739. http://dx.doi.org/10.1143/JJAP.27.L736.
5. Inoue A, Ohtera K, Tsai AP and Masumoto T. Aluminum-based amorphous alloys with tensile strength above 980 MPa (100

kg/mm ^{2}). *Japanese Journal of Applied Physics*. 1988; 27(4, Part 2):L479-L482. http://dx.doi.org/10.1143/JJAP.27.L479.

6. He Y, Poon SJ and Shiflet GJ. Synthesis and properties of metallic glasses that contain aluminum. *Science*. 1988; 241(4873):1640-1642. http://dx.doi.org/10.1126/science.241.4873.1640. PMid:17820894.
7. He Y, Dougherty GM, Shiflet GJ and Poon SJ. Unique metallic glass formability and ultra-high tensile strength in Al Ni Fe Gd alloys. *Acta Metallurgica et Materialia*. 1993; 41(2):337-343. http://dx.doi.org/10.1016/0956-7151(93)90064-Y.
8. He Y, Shiflet GJ and Poon SJ. Synthesis and properties of aluminum-based metallic glasses containing rare earths. *Journal of Alloys and Compounds*. 1994; 207–208:349-354. http://dx.doi.org/10.1016/0925-8388(94)90238-0.
9. Inoue A, Matsumoto N and Masumoto T. Al-Ni-Y-Co amorphous alloys with high mechanical strengths, wide supercooled liquid region and large glass-forming capacity. *Materials Transactions, JIM*. 1990; 31(6):493-500. http://dx.doi.org/10.2320/matertrans1989.31.493.
10. Tsai AP, Inoue A and Masumoto T. Ductile Al-Ni-Zr amorphous alloys with high mechanical strength. *Journal of Materials Science Letters*. 1988; 7(8):805-807. http://dx.doi.org/10.1007/BF00723766.
11. Tsai AP, Inoue A and Masumoto T. Formation of metal-metal type aluminum-based amorphous alloys. *Metallurgical Transactions A, Physical Metallurgy and Materials Science*. 1988; 19(5):1369-1371. http://dx.doi.org/10.1007/BF02662599.
12. Inoue A, Ohtera K and Masumoto T. Recent progress of aluminum base amorphous alloys. *Science reports of the Research Institutes, Series A, Physics, chemistry and metallurgy*. 1990; 35(1):115-164.
13. Inoue A, Sobu S, Louzguine DV, Kimura H and Sasamori K. Ultrahigh strength Al-based amorphous alloys containing Sc. *Journal of Materials Research*. 2004; 19(5):1539-1543. http://dx.doi.org/10.1557/JMR.2004.0206.
14. Inoue A, Amiya K, Yoshii I, Kimura H and Masumoto T. Production of Al-based amorphous alloy wires with high tensile strength by a melt extraction method. *Materials Transactions, JIM*. 1994; 35(7):485-488. http://dx.doi.org/10.2320/matertrans1989.35.485.
15. Oguchi M, Inoue A, Yamaguchi H and Masumoto T. Production of Al-based amorphous sheets with large thickness by a supercooled liquid-quenching method. *Journal of Materials Science Letters*. 1991; 10(5):289-291. http://dx.doi.org/10.1007/BF00735660.
16. Inoue A, Oguchi M, Yamaguchi H and Masumoto T. Aluminum-base amorphous powders with flaky morphology prepared by a two-stage quenching technique. *Materials Transactions, JIM*. 1989; 30(12):1033-1043. http://dx.doi.org/10.2320/matertrans1989.30.1033.
17. Inoue A, Oguchi M and Masumoto T. Study on the production of flaky amorphous alloy powders by impact flattening of atomized liquid droplets on a rapidly rotating wheel. *Science reports of the Research Institutes, Series A, Physics, chemistry and metallurgy*. 1993; 38(1):112-128.
18. Hishida M, Fujita M and Sakaki K. Fabrication of aluminum coating with dispersed nanoscale quasicrystalline particles by cold spray. *Journal of the Japan Institute of Metals and Materials*. 2009; 73(6):421-428. http://dx.doi.org/10.2320/jinstmet.73.421.
19. Inoue A, Onoue K, Horio Y and Masumoto T. Production of Al-based amorphous alloys by a metallic mold casting method and their thermal stability. *Science reports of the Research Institutes, Series A, Physics, chemistry and metallurgy*. 1994; 39(2):155-158.
20. Inoue A, Onoue K and Masumoto T. Microstructure and properties of bulky $Al_{84}Ni_{10}Ce_6$ alloys with amorphous surface layer prepared by high-pressure die casting. *Materials Transactions, JIM*. 1994; 35(11):808-813. http://dx.doi.org/10.2320/matertrans1989.35.808.
21. Zhuo W and Yong-Xiang L. Improvement in dielectric tunability of $Ba_{0.6}Sr_{0.4}TiO_4$-Mg_2TiO_4 composite ceramics via heterogeneous nucleation processing. *Chinese Physics Letters*. 2009; 26(11):066402. http://dx.doi.org/10.1088/0256-307X/26/11/117701.
22. Wang JQ, Liu YH, Imhoff S, Chen N, Louzguine-Luzgin DV, Takeuchi A, et al. Enhance the thermal stability and glass forming ability of Al-based metallic glass by Ca minor-alloying. *Intermetallics*. 2012; 29:35-40. http://dx.doi.org/10.1016/j.intermet.2012.04.009.
23. Kim YH, Inoue A and Masumoto T. Ultrahigh tensile strengths of $Al_{88}Y_2Ni_9M_1$ (M=Mn or Fe) amorphous alloys containing finely dispersed fcc-Al particles. *Materials Transactions, JIM*. 1990; 31(8):747-749. http://dx.doi.org/10.2320/matertrans1989.31.747.
24. Kim YH, Inoue A and Masumoto T. Ultrahigh mechanical strengths of $Al_{88}Y_2Ni_{10-x}M_x$ (M=Mn, Fe or Co) amorphous alloys containing nanoscale fcc-Al particles. *Materials Transactions, JIM*. 1991; 32(7):599-608. http://dx.doi.org/10.2320/matertrans1989.32.599.
25. Inoue A, Horio Y, Kim Y and Masumoto T. Elevated-temperature strength of an $Al_{88}Ni_9Ce_2Fe_1$ amorphous alloy containing nanoscale fcc-Al particles. *Materials Transactions, JIM*. 1992; 33(7):669-674. http://dx.doi.org/10.2320/matertrans1989.33.669.
26. Hono K, Zhang Y, Tsai AP, Inoue A and Sakurai T. Solute partitioning in partially crystallized Al-Ni-Ce(-Cu) metallic glasses. *Scripta Metallurgica et Materialia*. 1995; 32(2):191-196. http://dx.doi.org/10.1016/S0956-716X(99)80035-1.
27. Louzguine-Luzgin DV and Inoue A. Observation of linear defects in Al particles below 7 nm in size. *Journal of Materials Research*. 2006; 21(06):1347-1350. http://dx.doi.org/10.1557/jmr.2006.0189.
28. Zhuo L, Yang B, Wang H and Zhang T. Spray formed Al-based amorphous matrix nanocomposite plate. *Journal of Alloys and Compounds*. 2011; 509(18):L169-L173. http://dx.doi.org/10.1016/j.jallcom.2011.02.125.
29. Ohtera K, Inoue A, Terabayashi T, Nagahama H and Masumoto T. Mechanical properties of an $Al_{88.5}Ni_8Mm_{3.5}$ (Mm: Misch Metal) alloy produced by extrusion of atomized amorphous plus fcc-Al phase powders. *Materials Transactions, JIM*. 1992; 33(8):775-781. http://dx.doi.org/10.2320/matertrans1989.33.775.
30. Higashi K. Positive exponent superplasticity in advanced aluminum alloys with nano or near-nano scale grained structures. *Materials Science and Engineering A*. 1993; 166(1-2):109-118. http://dx.doi.org/10.1016/0921-5093(93)90315-6.
31. Taketani K, Uoya A, Ohtera K, Uehara T, Higashi K, Inoue A, et al. Readily superplastic forging at high strain rates in an aluminium-based alloy produced from nanocrystalline powders. *Journal of Materials Science*. 1994; 29(24):6513-6517. http://dx.doi.org/10.1007/BF00354013.
32. Nagahama H, Ohtera K, Higashi K, Indue A and Masumoto T. Mechanical properties of rapidly solidified aluminium alloys extruded from amorphous or nanocrystalline powders. *Philosophical Magazine Letters*. 1993; 67(4):225-230. http://dx.doi.org/10.1080/09500839308240933.
33. Hashikura M, Kaji T, Hattori H, Takikawa T, Takeda Y, Masumoto T, et al. Microstructure and mechanical properties of Al-Zr-Ni-RE (RE: Rare Earth Metal) alloys. In: *Proceedings of the 2000 Powder Metallurgy World Congress*; 2000; Kyoto, Japan. Kyoto: Japan Society of Powder and Powder Metallurgy; 2000. p. 1092-1095.

34. Inoue A and Kimura H. High elevated-temperature strength of Al-based nanoquasicrystalline alloys. *Nanostructured Materials*. 1999; 11(2):221-231. http://dx.doi.org/10.1016/S0965-9773(99)00035-5.

35. Huttunen-Saarivirta E. Microstructure, fabrication and properties of quasicrystalline Al–Cu–Fe alloys: a review. *Journal of Alloys and Compounds*. 2004; 363(1-2):154-178. http://dx.doi.org/10.1016/S0925-8388(03)00445-6.

36. Inoue A, Kimura H, Watanabe M and Masumoto T. Effect of additional M elements on bcc-Fe precipitation in Fe-Si-B-M (M=Nb, Zr or V) amorphous alloys. *Transactions of the Materials Research Society of Japan*. 1994; 16A(3):135-138.

37. A. Inoue, H. Kimura. High-strength Al-based alloys consisting mainly of nanoscale quasicrystalline or amorphous particles. *Materials Science Forum*. 1996, 235-238: 873-880.

38. Murty B, Ping D, Hono K, Kimura H and Inoue A. Microstructure of Rapidly Solidified High Strength $Al_{94}V_4Fe_2$ Alloy. *Materials Transactions*. 2003; 44(10):1993-1998. http://dx.doi.org/10.2320/matertrans.44.1993.

39. Kimura HM, Sasamori K and Inoue A. Al-Fe-based bulk quasicrystalline alloys with high elevated temperature strength. *Journal of Materials Research*. 2000; 15(12):2737-2744. http://dx.doi.org/10.1557/JMR.2000.0392.

40. Inoue A, Kimura H, Sasamori K and Masumoto T. Microstructure and mechanical properties of rapidly solidified Al-Cr-Ce-M (M=transition metal) alloys containing high volume fraction of the icosahedral phase. *Materials Transactions, JIM*. 1995; 36(1):6-15. http://dx.doi.org/10.2320/matertrans1989.36.6.

41. Inoue A, Kimura HM and Zhang T. High-strength aluminum- and zirconium-based alloys containing nanoquasicrystalline particles. *Materials Science and Engineering A*. 2000; 294–296:727-735. http://dx.doi.org/10.1016/S0921-5093(00)01307-1.

42. Inoue A, Kimura H and Amiya K. Bulk amorphous, nano-crystalline and nano-quasicrystalline alloys. IV. developments of aluminum- and magnesium-based nanophase high-strength alloys by use of melt quenching-induced metastable phase. *Materials Transactions*. 2002; 43(8):2006-2016. http://dx.doi.org/10.2320/matertrans.43.2006.

43. Kimura H, Inoue A and Sasamori K. Microstructure and mechanical properties of P/M P/M Al-V-Fe and Al-Fe-M-Ti (M = V, Cr, Mn) alloys containing dispersed quasicrystalline particles. *Materials Transactions, JIM*. 2000; 41(11):1550-1554. http://dx.doi.org/10.2320/matertrans1989.41.1550.

44. Hishida M, Fujita M and Sakaki K. Fabrication of aluminum coating with dispersed nanoscale quasicrystalline particles by cold spray. Journal of the Japan Institute of Metals and Materials. 2009; 73(6):421-428. http://doi.org/10.2320/jinstmet.73.421.

45. Grushko B and Velikanova TY. Stable and metastable quasicrystals in Al-based alloy systems with transition metals. *Journal of Alloys and Compounds*. 2004; 367(1-2):58-63. http://dx.doi.org/10.1016/j.jallcom.2003.08.012.

46. Ali F, Scudino S, Liu G, Srivastava VC, Mukhopadhyay NK, Samadi Khoshkhoo M, et al. Modeling the strengthening effect of Al-Cu-Fe quasicrystalline particles in Al-based metal matrix composites. *Journal of Alloys and Compounds*. 2012; 536(S1):S130-S133. http://dx.doi.org/10.1016/j.jallcom.2011.12.022.

47. Boudard M. Structural themes in approximant and decagonal quasicrystalline phases in Al based alloys. *Journal of Alloys and Compounds*. 2010; 495(2):365-371. http://dx.doi.org/10.1016/j.jallcom.2009.10.063.

48. Stan K., Lityńska-Dobrzyńska L., Lábár J.L. and Góral A. Effect of Mo on stability of quasicrystalline phase in Al-Mn-Fe alloy. *Journal of Alloys and Compounds*, 2014; 586(Suppl 1):S395-S399.

49. Dudina D.V., Georgarakis K., Aljerf M., Li Y., Braccini M., Yavari A.R., et al. Cu-based metallic glass particle additions to significantly improve overall compressive properties of an Al alloy. *Composites Part A: Applied Science and Manufacturing*. 2010; 41(10):1551-1557.

50. Fujii H, Sun Y, Inada K, Ji Y, Yokoyama Y, Kimura H, et al. Fabrication of Fe-based metallic glass particle reinforced Al-based composite materials by friction stir processing. *Materials Transactions*. 2011; 52(8):1634-1640. http://dx.doi.org/10.2320/matertrans.M2011094.

51. Aljerf M, Georgarakis K, Louzguine-Luzgin D, Le Moulec A, Inoue A and Yavari AR. Strong and light metal matrix composites with metallic glass particulate reinforcement. *Materials Science and Engineering A*. 2012; 532:325-330. http://dx.doi.org/10.1016/j.msea.2011.10.098.

52. Sasaki H, Kita K, Nagahora J and Inoue A. Nano-metals I. Nanostructures and mechanical properties of bulk Al-Fe alloys prepared by electron-beam deposition. *Materials Transactions*. 2001; 42(8):1561-1565. http://dx.doi.org/10.2320/matertrans.42.1561.

53. Sasaki H, Kobayashi N, Kita K, Nagahora J and Inoue A. Nanocrystalline structure and mechanical properties of vapor quenched Al-Zr-Fe alloy sheets prepared by electron-beam deposition. *Materials Transactions*. 2003; 44(10):1948-1954. http://dx.doi.org/10.2320/matertrans.44.1948.

54. Mukai T, Suresh S, Kita K, Sasaki H, Kobayashi N, Higashi K, et al. Nanostructured Al-Fe alloys produced by e-beam deposition: static and dynamic tensile properties. *Acta Materialia*. 2003; 51(14):4197-4208. http://dx.doi.org/10.1016/S1359-6454(03)00237-4.

55. Sakurai M, Matsuura M, Kita K, Sasaki H, Nagahora J, Kamiyama T, et al. EXAFS and SAXS analysis for nano-structural origin of high strength for supersaturated $Al_{100-x}Fe_x$ (x = 1, 2.5) alloys. *Materials Science and Engineering A*. 2004; 375-377:1224-1227. http://dx.doi.org/10.1016/j.msea.2003.10.166.

56. Inoue A, Yamagata H and Masumoto T. Nitrogen-induced amorphization in $Al_{80}Ti_{20}$ films prepared by reactive sputtering. *Materials Letters*. 1993; 16(4):181-184. http://dx.doi.org/10.1016/0167-577X(93)90159-U.

57. Inoue A, Yamagata H and Masumoto T. Production and properties of functionally gradient films varying from amorphous Al(Ti, N) to hexagonal Al(Ti)N phase. *Materials Transactions, JIM*. 1993; 34(6):548-555. http://dx.doi.org/10.2320/matertrans1989.34.548.

58. Yamagata H, Inoue A and Masumoto T. Functionally graded Al Zr-based amorphous alloys. *Materials Science and Engineering A*. 1994; 181–182:1300-1304. http://dx.doi.org/10.1016/0921-5093(94)90851-6.

59. Tokuoka T, Kaji T, Nishioka T and Ikegaya A. Development of high-strength, heat-resistant aluminum alloy made by powder forging process. *SEI Technical Review*. 2006; 61(1):70-76.